Effect of CO2 enrichment and increased nitrogen supply on the induction of sunflower (Helianthus annuus L.) primary leaf senescence

Authors: Canales, F.J., de la Haba, P., Barrientos, E., and Agüera, E.

Source: Canadian Journal of Plant Science, 96(6) : 1002-1013

Published By: Canadian Science Publishing

URL: https://doi.org/10.1139/cjps-2016-0124

NRC Research Press

ARTICLE

Effect of CO_2 enrichment and increased nitrogen supply on the induction of sunflower (*Helianthus annuus* L.) primary leaf senescence

F.J. Canales, P. de la Haba, E. Barrientos, and E. Agüera

Abstract: A study was made of the effect of atmospheric CO_2 enrichment and increased nitrogen availability on primary leaf senescence in sunflower (*Helianthus annuus* L.). First, markers normally used for monitoring leaf development (dry weight, leaf surface area, protein content, photosynthetic pigment levels, CO_2 fixation rate, changes in the enzymes involved in nitrogen metabolism, and plant-tissue oxidative status) were measured in plants grown for 42 days under ambient (400 μL L^{-1}) or enriched CO_2 conditions (800 μL L^{-1}), and with two different levels of nitrate supply (10 mM and 25 mM). Second, two-dimensional electrophoresis (2-DE) was used to compare primary-leaf protein profiles (16 and 42 days) in sunflowers grown under ambient or enriched CO_2 conditions with elevated nitrate supply. Plants grown under enriched CO_2 conditions and with high nitrogen supply displayed faster growth, a higher CO_2 fixation rate, and increased activity by antioxidative and nitrogen-metabolism-related enzymes than those grown under elevated CO_2 with low nitrogen supply. These findings indicate that CO_2 enrichment and increased nitrate availability slow down the induction of senescence, suggesting that senescence may be directly related to leaf C/N ratio. These results enhance our understanding of the sunflower's response to increased atmospheric CO_2 levels, one of the environmental factors favoring climate change.

Key words: development, growth parameters, *Helianthus annuus* L., photosynthesis, proteins.

Résumé : Les auteurs ont examiné les effets de l'enrichissement de l'air avec du CO_2 et d'une plus grande disponibilité d'azote sur la sénescence des feuilles primaires du tournesol (*Helianthus annuus* L.). Ils ont d'abord mesuré les marqueurs qui servent habituellement à surveiller le développement du feuillage (poids sec, surface foliaire, teneur en protéines, concentration de pigments photosynthétiques, taux de fixation du CO_2, modification au niveau des enzymes qui interviennent dans le métabolisme de l'azote et bilan oxydatif des tissus végétaux) chez des plants cultivés pendant 42 jours dans des conditions ambiantes (400 μL de CO_2 par litre) ou enrichies (800 μL de CO_2 par litre), à deux taux d'application de nitrate (10 mM et 25 mM). Ensuite, ils ont recouru à l'électrophorèse bidimensionnelle pour comparer le profil protéinique des feuilles primaires (à 16 et à 42 jours) des tournesols cultivés dans l'un ou l'autre milieu, avec un apport élevé d'azote. Comparativement à celles cultivées dans un milieu pauvre en CO_2 et en azote, les plantes poussant dans un milieu enrichi de CO_2 avec un apport élevé d'azote se sont caractérisées par une croissance plus rapide, un meilleur taux de fixation du CO_2 et une activité supérieure des enzymes antioxydants et des enzymes liés au métabolisme de l'azote. Ces constatations indiquent que l'enrichissement avec du CO_2 et la disponibilité d'une quantité supérieure de nitrate ralentissent la sénescence, et que cette dernière pourrait être directement reliée au ratio C/N des feuilles. Ces résultats nous aident à comprendre comment le tournesol réagit à la hausse de la concentration de CO_2 dans l'atmosphère, un des facteurs environnementaux qui accélèrent le changement climatique. [Traduit par la Rédaction]

Mots-clés : développement, facteurs de croissance, *Helianthus annuus* L., photosynthèse, protéines.

Received 19 April 2016. Accepted 29 June 2016.

F.J. Canales, P. de la Haba, E. Barrientos, and E. Agüera. Departamento de Botánica, Ecología y Fisiología Vegetal, Área de Fisiología Vegetal, Facultad de Ciencias, Universidad de Córdoba, Campus de Rabanales, Edificio Celestino Mutis (C4), 3ª planta, E-14071 Córdoba, Spain.

Corresponding author: E. Agüera (email: vg1agbue@uco.es).

Introduction

The Intergovernmental Panel on Climate Change (IPCC) has predicted that CO_2 concentrations in the atmosphere may increase by 660–790 μL L^{-1} over the period 2060–2090 (IPCC 2007). Studies on various plant species have shown that climate change affects development, growth, and productivity through changes in biochemical, physiological, and morphogenetic processes (AbdElgawad et al. 2015). Elevated atmospheric CO_2 levels inhibit photorespiration in C3 plants, increasing their photosynthetic efficiency, as the carboxylation capacity of Rubisco (ribulose 1,5 bisphosphate carboxylase/oxygenase) is not saturated by the current CO_2 concentration (Drake et al. 1997). This enzyme, which is the most abundant protein on earth, accounts for a high proportion of all nitrogen in C3 plants (Feller et al. 2008). Elevated CO_2 concentrations are also known to increase CO_2 fixation rates (Agüera et al. 2006; de la Mata et al. 2012), and consequently, plant biomass production (AbdElgawad et al. 2015). However, a number of C3 species exhibit no such increase in biomass when elevated CO_2 concentrations prevail over long periods (Ainsworth et al. 2006); under these conditions, some plants exhibit decreased photosynthetic rates (Long et al. 2004) and the amounts of photoassimilates exported from source organs to sink organs are reduced in relation to plant photosynthetic capacity, eventually leading to increased sugars accumulation. Increased sugar levels can inhibit the genes coding for photosynthetic enzymes and diminish photosynthetic activity and plant or biomass production, resulting in a process known as "photosynthetic acclimation" (Ainsworth et al. 2006). The triggering of senescence may be one of the mechanisms involved in the photosynthetic acclimation response to elevated CO_2 concentrations. Leaf senescence is a key stage in the life of annual plants, during which they undergo marked metabolic changes and sequential degeneration of cell structures. Senescence is linked to major changes in the expression of certain genes, particularly those involved in photosynthesis; senescence down-regulated genes (SDGs), whose expression ceases, and senescence-associated genes (SAGs), which are induced. These genes act mainly by encoding degradation enzymes such as proteases, lipases, nucleases, and nitrogen- mobilizing enzymes (Buchanan-Wollaston et al. 2005). Senescence progresses with plant age, and is highly-regulated to prevent its occurring too early during a plant's life cycle; it appears to be triggered and regulated by both internal (C/N ratio, hormones) and external factors (light, availability of nutrients — particularly nitrogen, CO_2 concentrations, and biotic and abiotic stress) (Lim et al. 2007; Agüera et al. 2010). Elevated CO_2 concentrations can affect leaf senescence in various ways; some authors report that they expedite the process (de la Mata et al. 2012), whereas others have recorded the opposite effect (Tricker et al. 2004). de la Mata et al. (2013) observed that elevated atmospheric CO_2 concentrations during leaf development in sunflower (*Helianthus annuus* L.) lead to early senescence through a decrease in nitrogen content. Research in this area has focused on obtaining new cultivars capable of withstanding changing climatic conditions, on the grounds that elevated CO_2 concentrations affect nitrogen assimilation (Bloom et al. 2010).

The present study sought to examine the possible effect of increased nitrogen supply and elevated atmospheric CO_2 concentrations on the induction of primary leaf senescence in sunflower, and on the biochemical and physiological processes involved in leaf ontogeny.

Materials and Methods

Plant material and growth

Seeds of sunflower from the isogenic cultivar HA-89 (Semillas Cargill SA, Seville, Spain) were surface-sterilized in 1% (*v*/*v*) hypochlorite solution for 15 min. After rinsing in distilled water, the seeds were imbibed for 3 h and then sown (10 seeds) in plastic trays (40 cm × 30 cm × 25 cm) containing a 1:1 (*v*/*v*) mixture of perlite and vermiculite. Seeds were germinated and plants grown in a growth chamber (Sanyo Gallenkamp Fitotron, Leicester, UK) with a 16 h photoperiod (400 μmol m^{-2} s^{-1} of photosynthetically active radiation supplied by "cool white" fluorescent lamps supplemented by incandescent bulbs), a day/night temperature regime of 25 °C/19 °C and 70%/80% relative humidity. Plants were irrigated daily with a complete nutrient solution (Hewitt 1966) containing two different nitrate concentrations: 10 mM (control nitrate) or 25 mM (elevated nitrate); after 8 d, plants were transferred to different controlled environment cabinets (Sanyo Gallenkamp Fitotron, Leicester, UK) fitted with an ADC 2000 CO_2 gas monitor; they were kept there, under ambient CO_2 (400 μL L^{-1}) or elevated CO_2 concentrations (800 μL L^{-1}), for a further 34 d. High-purity CO_2 was supplied from a compressed gas cylinder (Air Liquide, Seville, Spain). Samples of primary leaves aged 16, 22, 32, and 42 d, counted from sowing, were collected 2 h after the light photoperiod was started. Whole leaves were excised and pooled in two groups. One group was used for dry weight (DW) and leaf surface area measurements, made with the Image Pro Plus image-analysis software program. The other group was immediately frozen in liquid nitrogen and stored at −80 °C. The frozen plant material was ground in a mortar pre-cooled with liquid N_2 and the resulting powder distributed into small vials that were stored at −80 °C until measurement of enzyme activity and metabolite levels.

Gas exchange

Net CO_2 fixation rate, transpiration, and stomatal conductance were measured 2 h after the start of the photoperiod in attached leaves, using a Portable Photosynthesis System (PP system, model CRSO68, Massachusetts, USA) controlled with CIRAS software.

Gas exchange rates were determined under 400 or 800 μL L^{-1} CO_2 levels. The instrument was adjusted to maintain 150 cm^3 min^{-1} constant flow, 25 °C temperature, 80% relative humidity, and 400 μmol m^{-2} s^{-1} lighting inside the leaf chamber. Measurements were made on primary leaves (16, 22, 32, and 42 d) after a stabilization period, using six plants per treatment. Leaf samples were acclimated in the leaf chamber for 5–10 min and measurements were carried out over the following 3–5 min.

Proteins, pigment and H_2O_2 determinations

Frozen material was homogenized with cold extraction medium (4 mL g^{-1}) consisting of 50 mM Hepes-KOH (pH 7), 5 mM $MgCl_2$, and 1 mM EDTA and analyzed with the Bio-Rad assay according to Bradford (1976). Pigments were determined in plant extracts by HPLC following Cabello et al. (1998). For H_2O_2 determination, 1 g leaf material was ground with 10 mL cool acetone in a cold room and passed through Whatman filter paper. H_2O_2 was determined by formation of the titanium–hydroperoxide complex following Mukherjee and Choudhuri (1983).

Enzymatic antioxidant activity

For determination of catalase (CAT) (E.C.1.11.1.6) and ascorbate peroxidase (APX) (E.C.1.11.1. 11), enzyme extracts were prepared by freezing a weighed amount of leaf samples in liquid nitrogen to prevent proteolytic activity, followed by grinding in 0.1 M phosphate buffer at pH 7.5 containing 0.5 mM EDTA and 1 mM ascorbic acid at a ratio of 1:10 (*w*/*v*). The homogenate was passed through four layers of gauze, the filtrate was centrifuged at 15 000*g* for 20 min, and the resulting supernatant was used as enzyme source. CAT activity was estimated following Aebi (1983). The reaction mixture contained 50 mM potassium phosphate (pH 7) and 10 mM H_2O_2. After addition of the enzyme, H_2O_2 decomposition was monitored via absorbance at 240 nm (ε = 43.6 mM^{-1} cm^{-1}). APX activity was measured following Nakano and Asada (1981). The reaction mixture contained 50 mM phosphate buffer (pH 7), 1 mM sodium ascorbate, and 25 mM H_2O_2. Following addition of the enzymatic extract to the mixture, the reaction was monitored via absorbance at 290 nm (ε = 2.8 mM^{-1} cm^{-1}). The CAT and APX activities were expressed U g^{-1} DW (U = μmol min^{-1}).

Extraction and activity of enzymes involved in nitrogen metabolism

Frozen material was homogenized in a chilled extraction medium (4 mL g^{-1}) consisting of 100 mM Hepes-KOH (pH 7.5), 10% (*v*/*v*) glycerol, 1% (*w*/*v*) polyvinylpolypyrrolidone (PVPP), 0.1% (*v*/*v*) Triton X-100, 6 mM dithiothreitol (DTT), 1 mM EDTA, 0.5 mM phenylmethylsulfonyl fluoride (PMSF), 25 μM leupeptin, 20 μM flavin adenine dinucleotide (FAD), and 5 μM Na_2MoO_4. The homogenate was centrifuged at 8000*g* at 4 °C for 2 min, and enzymes activities (NR and GS) were measured immediately using the cleared extract. NR (E.C. 1.6.6.1) activity was determined in the absence of Mg^{2+} to measure total NADH-NR activity. Nitrite formed was determined spectrophotometrically at 540 nm, following Agüera et al. (2006). GS (E.C. 6.3.1.2) activity was measured with the transferase assay in a reaction mixture containing, in a final volume of 1 mL, 50 mM Hepes–KOH (pH 7.5), 30 mM L-glutamine, 60 mM NH_2OH, 0.4 mM ADP, 3 mM $MnCl_2$, 20 mM Na_2HASO_4, and an adequate amount of enzyme preparation. The mixtures were incubated at 30 °C and the reactions terminated by addition of 2 mL of cold ferric-chloride reagent (120 mM $FeCl_3$, 78 mM HCl, and 73 mM trichloroacetic acid). The γ-glutamyl hydroxamate formed was determined spectrophotometrically at 500 nm, following de la Haba et al. (1992).

Protein extraction

Proteins were extracted from primary leaves (500 μg frozen powder) using the TCA (trichloroacetic acid)-acetone-phenol protocol recommended by Wang et al. (2006). The pellet recovered by centrifugation was rinsed with cold methanol and acetone dried under a nitrogen atmosphere for re-suspension in 100 μL of buffer containing: 7 M urea, 4% (*w*/*v*) 3-[(3-cholamidopropyl)dimethylammonio]-1-propanesulfonate (CHAPS), 2% Triton X-100, 100 mM DTT, and 2% (*v*/*v*) IPG Buffer pH 3–10. Lipids and nucleic acids were removed by ultracentrifugation for 30 min at 4 °C at 9740*g* (5415 R Eppendorf), and the protein content in the supernatant was quantified by the Bradford method, as modified by Ramagli and Rodriguez (1985), using BSA as standard. Samples were stored at −80 °C until electrophoresis.

Two dimensional electrophoresis (2-DE), gel staining, image capture, and analysis

Precast 7 cm non-linear pH 3–10 strips (BioRad) were rehydrated for 6 h with 170 μg of proteins in 125 μg of rehydration buffer containing 9 mol L^{-1} urea, 4% (*w*/*v*) CHAPS, 20 mM DTT, 2% Ampholites (Biolyte 3/10, BioRad), and 0.005% bromophenol blue. IEF (isoelectrofocusing-BioRad Protean IEF Cell system) was carried out at 20 °C at a gradually increasing voltage: 0–50 V for 6 h, 50–250 V for 1 h, 250–4000 V for 2 h, and to 15 000 V for 1 h with a maximum voltage of 4000 V h. After IEF, IPG (immobilized pH gradient) strips were equilibrated according to Gorg et al. (1988) by immersing them first in 375 mM Tris–HCl, pH 8.8, containing 6 mol L^{-1} urea, 2% SDS (sodium dodecyl sulfate), 20% glycerol, and 2% DTT, and then in the same solution containing 2.5% iodoacetamide instead of DTT. The strips were then transferred onto vertical slab 12% SDS-polyacrylamide gels (Bio-Rad PROTEAN Plus Dodeca Cell) and electrophoresis was run at 100 V for 1 h and at 60 V until the dye front reached the gel bottom. Gels were stained with Comassie Brillant Blue (CBB) G-250 (Bio-Rad)

(Heazlewood and Millar 2003). Gel images were obtained using a SHRP JX-330 scanner and GS800 densitometer (BioRad) and analyzed with PD QuestTM software (BioRad), using a 10-fold over background as minimum criterion for spot presence or absence. Results were re-assessed by visual inspection. Normalized spot volumes (individual spot intensity/normalization factors as calculated for each gel from the total number of valid spots) were determined for each individual spot and these values were used to designate significant differentially-expressed spots. Only those spots exhibiting statistically-significant differences ($P < 0.05$) in intensity, in terms of Student's t-test, were considered for further analysis.

MALDI-TOF/TOF MS and protein identification

Spots from CBB-stained gels were excised automatically in a ProPic station (Genomic Solutions, UK), digested with modified porcine trypsin (sequencing grade; Promega) and loaded onto the MALDI plate using a ProPrep II station (Digilab Genomic Solutions Inc., UK). Gel specimens were destained twice with 200 mM ammonium bicarbonate/40% acetonitrile at 37 °C over 30 min. Gel pieces were then subjected to three consecutive dehydration/rehydration cycles with pure acetonitrile and 25 mM ammonium bicarbonate in 50% acetonitrile, respectively, and finally dehydrated with pure acetonitrile for 5 min and dried out at room temperature for 4 h. Then 20 μL trypsin, at a concentration of 12.5 ng μL^{-1} in 25 mM ammonium bicarbonate, was added to the dry gel pieces and digestion took place at 37 °C for 12 h. Peptides were extracted from gel plugs by adding 1 μL of 10% (*v*/*v*) TFA (trifluoroacetic acid) and incubating for 15 min. They were then desalted, and concentrated using μC-18 ZipTip columns (Millipore), and directly loaded onto the MALDI plate using α-cyano hydroxycinnamic acid as matrix. Mass spectrometry (MS) analysis of peptides in each sample was performed with a Matrix Assisted Laser Desorption Ionization-Time-of-Flight (MALDI-TOF/TOF; 4800 Proteomics Analyzer, Applied Biosystems) mass spectrometer over the m/z range 800–4000, with an accelerating voltage of 20 kV. Spectra were internally calibrated with peptides from trypsin autolysis (M+H+=842.509, M+H+=2211.104) and the most abundant peptide ions were then subjected to fragmentation analysis (MS/MS) to elucidate the peptide sequence. Proteins were assigned identification by peptide mass fingerprinting (PMF) and confirmed by MS/MS analysis. The Mascot 2.0 search engine (Matrix Science Ltd., London, UK; http://www.matrixscience.com) was used for protein identification running on GPS Explorer™ software v3.5 (Applied Biosystems, Foster City, CA, USA) over non-redundant NCBI protein and Uniprot databases. Search settings allowed one missed cleavage with the selected trypsin enzyme, a MS/MS fragment tolerance of 0.2 Da, a precursor mass tolerance of 100 ppm, and cysteine carbamidomethylation and methionine oxidation as possible modifications. Only proteins matched with >99% confidence by a minimum of 7 peptide sequences were included in the results list. Proteins with statistically-significant ($P < 0.05$) hits were positively assigned identification after considering Mr and pI values.

Statistical analysis

Results are presented as means ± SD of three independent experiments performed sequentially using duplicated determination in each experiment. One-way analyses of variance (ANOVA) were performed on the original data to evaluate the effect of CO_2 and nitrate treatments on different sampling days. Pair-wise comparisons of means were made using Tukey's test; differences were considered statistically significant at $P < 0.05$. Results for 2-DE are the means ± SD from three separate experiments and the all data were additionally subjected to Student's t-test at a significance level of 5% ($P < 0.05$).

Results and Discussion

Leaf senescence involves a complex interplay between internal and external factors, which determine the timing, progression, and completion of senescence. Under optimal growth conditions, the onset of leaf senescence occurs in an age-dependent manner (Schippers et al. 2015). During its lifetime, a plant is exposed to various environmental conditions that can prematurely induce the senescence program. To study the effect of CO_2 enrichment and increased nitrogen availability on the induction of sunflower primary-leaf senescence, markers normally used for monitoring leaf development (dry weight, leaf area, protein content, photosynthetic pigment levels, CO_2 fixation rate, changes in the enzymes involved in nitrogen metabolism, and plant-tissue oxidative status) were measured in the primary leaves of sunflower plants grown for 42 d with control (10 mM) or high (25 mM) nitrate concentrations and ambient CO_2 (400 μL L^{-1}) or enriched CO_2 conditions (800 μL L^{-1}). Subsequently, two-dimensional electrophoresis (2-DE) was used to compare primary-leaf protein profiles (at 16 and 42 d growth) in sunflowers grown under ambient or enriched CO_2 conditions with elevated nitrate supply.

Results indicated that DW and leaf area increased under elevated CO_2 conditions, especially in plants grown with increased nitrate availability (25 mM); a synergic effect of the two factors was observed throughout leaf development (Figs. 1A, 1B). A similar study on *Arabidopsis* found that when plants were grown under elevated CO_2 (780 μL L^{-1}) and sufficient N (30 mM), plant growth was dramatically promoted and leaves were enlarged (Aoyama et al. 2014). It has been reported that elevated atmospheric CO_2 concentrations may influence both cell division (Kinsman et al. 1997) and expansion

Fig. 1. Changes in dry weight (DW) (A), leaf area (B), and soluble protein (C) during sunflower primary leaf development. Plants were grown under different treatments: 10 mM NO_3^-/400 μL $L^{-1}CO_2$; 10 mM NO_3^-/800 μL L^{-1} CO_2; 25 mM NO_3^-/400 μL L^{-1} CO_2; 25 mM NO_3^-/800 μL L^{-1} CO_2. Data are means ± SD of duplicate determinations from three separate experiments. Bars followed by different letters show significant difference among the treatments according to Tukey's test ($P < 0.05$).

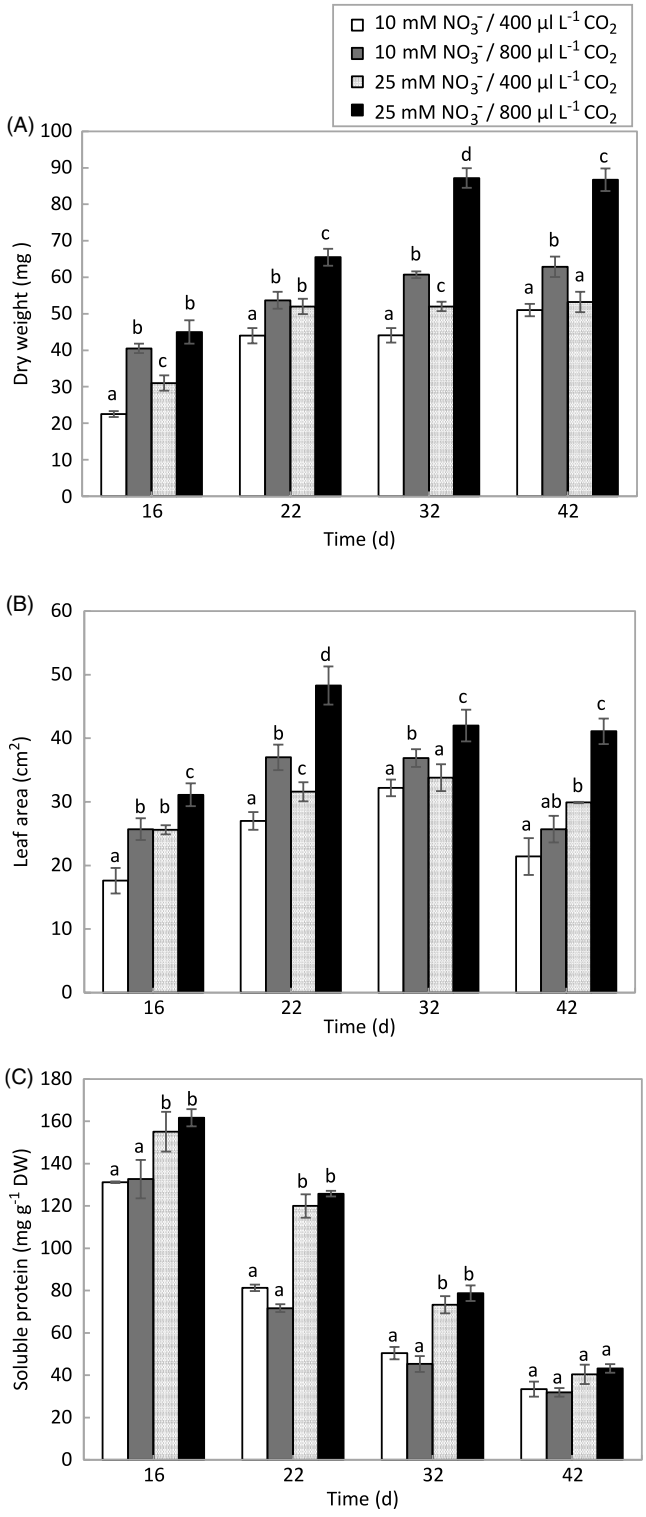

(Taylor et al. 2003; Kontunen-Soppela et al. 2010; Riikonen et al. 2010). Leaf size is determined by cell division and expansion, which are controlled in a coordinated manner during organogenesis by a complex network of factors, including plant hormones, in response to environmental cues (Nishimura et al. 2004; Tsukaya 2006; Riikonen et al. 2010).

A significant decrease in soluble protein content (approximately 75%) was observed during ageing of sunflower primary leaves under all treatments; however, elevated nitrate availability significantly increased protein levels (about 50% in mature leaves) under both ambient CO_2 (400 μL L^{-1}) and enriched CO_2 conditions (800 μL L^{-1}) (Fig. 1C). Protein degradation occurs through the action of proteases and via the ubiquitin-proteasome system. At least a portion of senescence-associated proteases localizes to senescence-associated vacuoles to degrade chloroplast-derived proteins (Carrion et al. 2013; Schippers et al. 2015). Aoyama et al. (2014) report that under conditions of elevated CO_2 and sufficient nitrogen, *Arabidopsis* plants produced greater amounts of organic compounds such as proteins for plant growth.

Photosynthetic pigment content was lower in plants grown under enriched CO_2 conditions than in those grown under ambient CO_2 (Fig. 2A). Leaf ageing reduced photosynthetic pigment content under all treatments: in plants grown with 10 mM nitrate, total chlorophyll content decreased by about 57% between 22 and 42 d under enriched CO_2 conditions, but only by 30% under ambient atmospheric CO_2 conditions. However, total chlorophyll content fell by about 40% between 22 and 42 d in plants grown with elevated nitrate availability (25 mM) under both CO_2 conditions (400 and 800 μL L^{-1}) (Fig. 2A). These results suggest that elevated CO_2 conditions accelerate chlorophyll degradation, and possibly also leaf senescence, when nitrogen availability is lower (10 mM). Likewise, in the course of leaf development, carotenoid content decreased by around 60% in plants grown under elevated CO_2 concentrations, but only about by 40% in those grown under ambient CO_2 in both nitrate treatments (10 and 25 mM), i.e., carotenoid degradation during ontogeny was more marked under elevated CO_2 conditions, regardless of nitrogen availability. Elevated CO_2 decreases photorespiration, a process through which excess reducing power is partly dissipated, and may thus damage the photosynthetic apparatus, leading to a decreases in photosynthetic pigments (Taniguchi and Miyake 2012). Photorespiration has been shown to maintain redox homeostasis within plant cells (Scheibe and Dietz 2012).

H_2O_2 production and the activity of antioxidant enzymes catalase and APX were also studied in sunflower leaves. As Fig. 3A shows, H_2O_2 production increased with leaf ageing, especially under elevated CO_2 conditions and with control nitrogen availability (10 mM); however, increased nitrogen supply (25 mM) in plants grown under elevated CO_2 conditions, prompted

Fig 2. Changes in Total chlorophyll (A), carotenoids (B) levels during sunflower primary leaf development. Plants were grown under different treatments: 10 mM NO_3^-/400 μL L^{-1} CO_2; 10 mM NO_3^-/800 μL L^{-1} CO_2; 25 mM NO_3^-/400 μL L^{-1} CO_2; 25 mM NO_3^-/800 μL L^{-1} CO_2. Data are means ± SD of duplicate determinations from three separate experiments. Bars followed by different letters show significant difference among the treatments according to Tukey's test ($P < 0.05$).

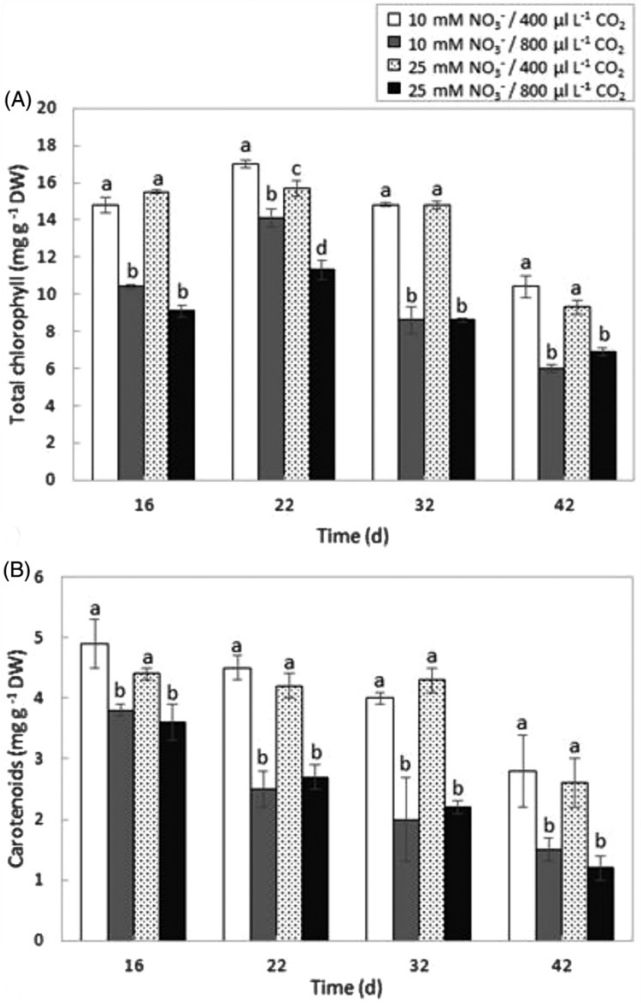

a decrease in H_2O_2 levels. Elevated CO_2 decreased CAT and APX activities, especially in plants grown under low nitrate availability conditions (Figs. 3B, 3C). de la Mata et al. (2012) reported that elevated levels of CO_2 may play a role in regulating leaf senescence in sunflower plants by increasing reactive oxygen species (ROS) production. Photosynthesis generates highly reactive compounds as it captures solar energy and converts it into energy-rich, but stable, compounds such as carbohydrates. Metabolic pathways, especially under stressful conditions, may become unbalanced, and dangerous compounds such as ROS may accumulate (Voss et al. 2013). These findings suggest that exposure of sunflower plants to elevated CO_2 conditions and elevated nitrogen availability decreases oxidative stress by lowering ROS

Fig. 3. H_2O_2 content (A), catalase (B), and APX (C) activities, during sunflower primary leaf development. Plants were grown under different treatments: 10 mM NO_3^-/400 μL L^{-1} CO_2; 10 mM NO_3^-/800 μL L^{-1} CO_2; 25 mM NO_3^-/400 μL L^{-1} CO_2; 25 mM NO_3^-/800 μL L^{-1} CO_2. Data are means ± SD of duplicate determinations from three separate experiments. Bars followed by different letters show significant difference among the treatments according to Tukey's test ($P < 0.05$).

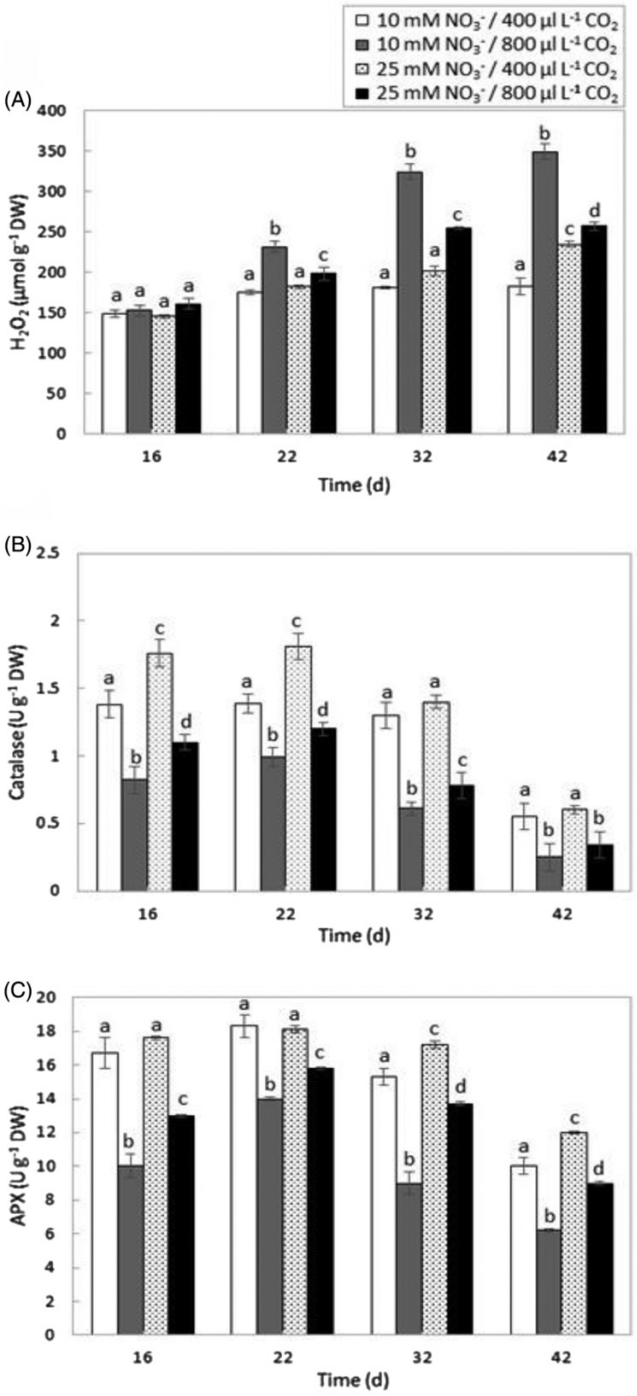

(H_2O_2) levels and increasing the activity of antioxidant enzymes such as catalase and APX compared with plants grown under elevated CO_2 and low N availability.

Fig. 4. CO_2 fixation rate (A), transpiration rate (B), and stomatal conductance (C) during sunflower primary leaf development. Plants were grown under different treatments: 10 mM NO_3^-/400 μL L^{-1} CO_2; 10 mM NO_3^-/800 μL L^{-1} CO_2; 25 mM NO_3^-/400 μL L^{-1} CO_2; 25 mM NO_3^-/800 μL L^{-1} CO_2. Data are means ± SD of duplicate determinations from three separate experiments. Bars followed by different letters show significant difference among the treatments according to Tukey's test ($P < 0.05$).

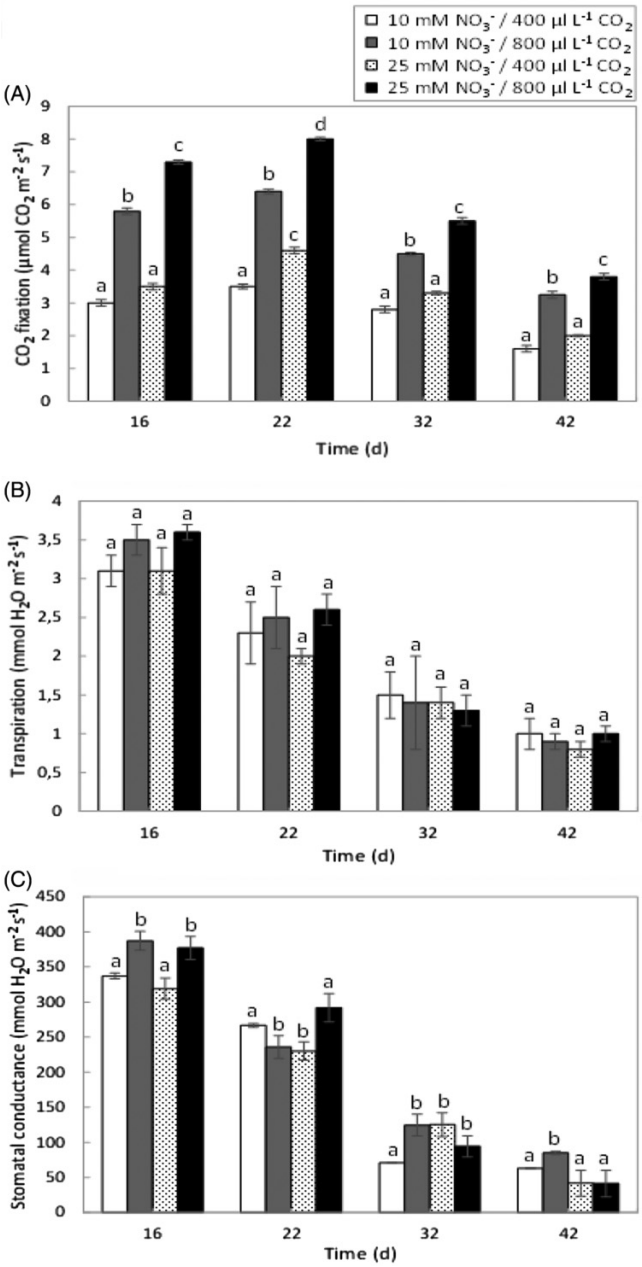

Nutrient availability, in particular that of carbon and nitrogen, is one of the most important factors for the regulation of plant metabolism and development. In sunflower plant leaves, the carbon dioxide fixation rate was negatively affected by ageing, after 22 d, in all treatments (Fig. 4A), being higher throughout the whole

Fig. 5. NR (A) and GS (B) activities, during sunflower primary leaf development. Plants were grown under different treatments: 10 mM NO_3^-/400 μL $L^{-1}CO_2$; 10 mM NO_3^-/800 μL L^{-1} CO_2; 25 mM NO_3^-/400 μL L^{-1} CO_2; 25 mM NO_3^-/800 μL L^{-1} CO_2. Data are means ± SD of duplicate determinations from three separate experiments. Bars followed by different letters show significant difference among the treatments according to Tukey's test ($P < 0.05$).

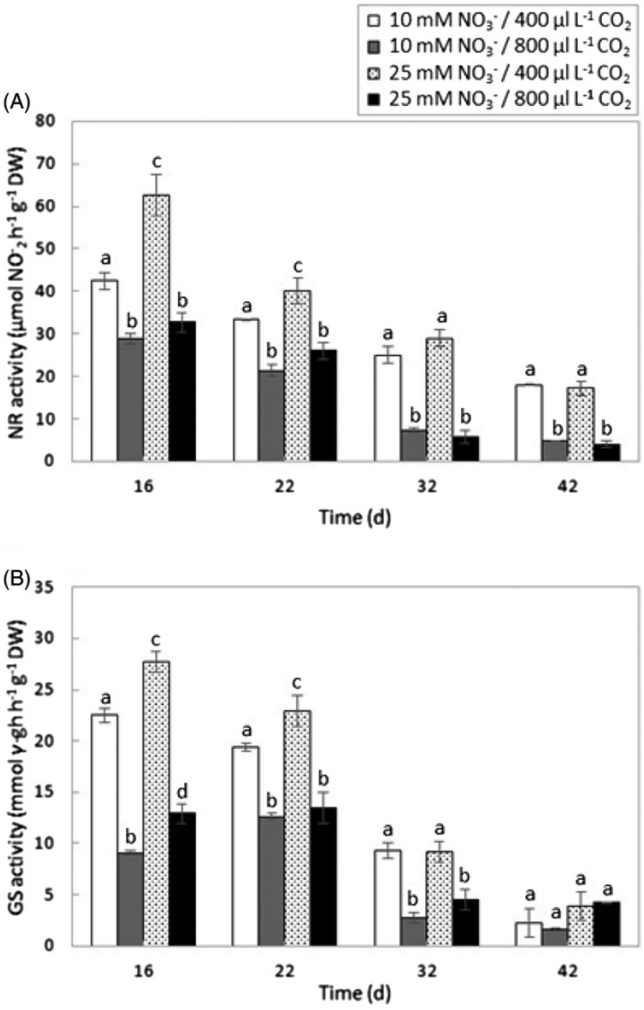

leaf-development period in plants grown under a CO_2 enriched atmosphere and with high nitrogen availability (25 mM); neither of these growing conditions affected transpiration rate and stomatal conductance, though both parameters decreased during leaf ontogeny (Figs. 4B, 4C). Plants grown under elevated CO_2 concentration exhibited significantly ($P < 0.05$) lower NR and GS activities (Fig. 5) than those grown under ambient atmospheric CO_2 conditions in both nitrate treatments (10 and 25 mM) and throughout development. Elevated CO_2 inhibits shoot nitrogen assimilation in C3 plants through two different mechanisms: (1) elevated CO_2 inhibits nitrite transport into chloroplasts; (2) elevated CO_2 inhibits the photorespiration process (Bloom et al. 2010). Photorespiration stimulates the export of malate

Table 1. Identification of differential spot proteins by MALDI-TOF/TOF and classification according to their functions.

Spot[a]	Ratio[b,c]	*P* value	Protein name (species) accession code[d]	MASCOT score/MP[e]	Mr/pI[f] experimental (theoretical)	% Coverage/ total ion score	Function
3	−1.35 *16T/16C* 1.23 *42T/42C* −7.33 *42C/16C* −4.39 *42T/16T*	0.074 0.166 0.008 0.007	At1g76940 (*Arabidopsis thaliana* — A1A6K6)	64/9	19700/5.00 (25575/8.83)	55/—	Nucleic acid binding
1003	−1.01 *16T/16C* −1.05 *42T/42C* −1.03 *42C/16C* −1.07 *42T/16T*	0.764 0.517 0.587 0.375	Chloroplast light-harvesting chlorophyll a/b-binding protein (Fragment) (*Artemisia annua* — A5HSG6)	360/11	19300/5.50 (26996/5.32)	30/318	Photosynthesis
3604	2.04 *16T/16C* 2.38 *42T/42C* −6.47 *42C/16C* −5.54 *42T/16T*	0.036 0.008 0.016 0.021	Rubisco subunit binding-protein β subunit (*Ricinus communis* — B9SBN5)	472/20	63900/5.60 (64491/5.65)	31/368	Photosynthesis
1406	1.42 *16T/16C* 1.60 *42T/42C* −4.20 *42C/16C* −3.73 *42T/16T*	0.041 0.001 0.011 0.011	Rubisco activase (*Flaveria bidentis* — A8W9B0)	731/32	40100/5.40 (48808/6.10)	52/561	Photosynthesis
1505	1.27 *16T/16C* 1.80 *42T/42C* −4.28 *42C/16C* −3.02 *42T/16T*	0.153 0.004 0.003 0.020	Rubisco activase (*Cucumis sativus* — Q01587)	582/22	47400/5.30 (45909/7.57)	40/490	Photosynthesis
5502	1.44 *16T/16C* 2.58 *42T/42C* −3.06 *42C/16C* −1.71 *42T/16T*	0.013 0.005 0.001 0.004	Rubisco large subunit (Fragment) (*Helianthus annuus* — D3PFB6)	1000/46	51700/6.00 (52613/5.87)	59/665	Photosynthesis
2501	1.52 *16T/16C* 1.72 *42T/42C* −2.36 *42C/16C* −2.09 *42T/16T*	0.017 $3{\cdot}10^{-4}$ 0.022 0.001	ATP synthase subunit beta, chloroplastic (*Ageratina adenophora* — F6MHM6)	1120/42	52900/5.50 (53617/5.12)	72/858	Energy metabolism
8501	−2.17 *16T/16C* −2.45 *42T/42C* 2.34 *42C/16C* 2.08 *42T/16T*	$4{\cdot}10^{-4}$ $3.3{\cdot}10^{-3}$ $1.6{\cdot}10^{-5}$ 0.039	Serine hydroxymethyltransferase (*Oryza brachyantha* — J3LSN2)	543/28	54800/8.30 (56534/8.72)	29/432	Photorespiration
1401	1.10 *16T/16C* −1.03 *42T/42C* 6.58 *42C/16C* 5.84 *42T/16T*	0.697 0.801 0.001 0.009	Peptidyl-prolyl cis-trans isomerase, chloroplastic (*Spinacia oleracea* — O49939)	285/18	39200/5.20 (50069/5.29)	24/216	Foldase proteins
1705	1.04 *16T/16C* 1.64 *42T/42C* −2.95 *42C/16C* −1.87 *42T/16T*	0.624 0.051 0.003 0.007	Heat shock protein (*Ricinus communis* — B9SKC7)	732/28	80600/5.30 (75431/5.35)	33/573	Stress response

(*continued*).

Table 1. (*concluded*).

Spot[a]	Ratio[b,c]	*P* value	Protein name (species) accession code[d]	MASCOT score/MP[e]	Mr/pI[f] experimental (theoretical)	% Coverage/ total ion score	Function
2101	∞ *16T/16C*	0.000	Plastid-lipid-associated protein	258/8	22100/5.50 (23765/5.74)	27/226	Redox-stress related
	−0.92 *42T/42C*	0.621	(Fragment) (*Glycine max* — I1LC75)				
	729 *42C/16C*	0.017					
	674 *42T/16T*	0.000					
1101	∞ *16T/16C*	0.000	Plastid-lipid-Associated protein	205/7	23800/5.20 (29385/4.83)	24/178	Redox-stress related
	1.12 *42T/42C*	0.555	(Fragment) (*Nicotiana tabacum* —				
	748 *42C/16C*	0.021	O24141)				
	670 *42T/16T*	0.003					

[a]Spot number assigned by PD-Quest software.
[b]Data present average ratio ("+" or "−" sign, respectively, indicates an n-fold increase or decrease of the relative abundance protein in the compared conditions):
[c]16C (ambient CO_2 plants 16 d), 16T (elevated CO_2 plants 16 d), 42C (ambient CO_2 plants 42 d), 42T (elevated CO_2 plants 42 d).
[d]Accession number from Uniprot database.
[e]MP: matched peptides.
[f]Experimental Mr calculated using standard molecular weight markers and PD-Quest software and pI were calculated with PD-Quest software.

from the chloroplast into the cytoplasm, and this malate generates the NADH used to reduce nitrate to nitrite (Bloom et al. 2010, 2012; Aranjuelo et al. 2013; de la Mata et al. 2013; Lekshmy et al. 2013; Bloom 2015). Elevated CO_2 with limited N availability disrupts plant growth and gives rise to senescence progression, indicated by chlorosis, anthocyanin accumulation, and increased GS1 expression (de la Mata et al. 2013; Aoyama et al. 2014). A transcriptomic approach has recently shown that exposure to high CO_2 concentrations (800 μL L^{-1}) induces the expression of genes involved in the transport of nitrate, but leaf N and mineral status suggested limited N assimilation into proteins (Jauregui et al. 2016). Research in *Arabidopsis* has found that there is no visible senescence-promoting effect under either low CO_2/low N conditions or high CO_2/high N conditions at the same growth stage, concluding that the senescence phenotype observed is not due to limited levels of N or to elevated CO_2, but is dependent upon the CO_2/N ratio (Aoyama et al. 2014). An increase in atmospheric CO_2 levels disrupts the C/N balance, increasing C and reducing N, repressing the expression of photosynthesis-related genes and promoting the expression of stress-responsive genes (Aoyama et al. 2014). Enhanced nitrate supply can reverse senescence processes, affecting the genes coding for various enzymes (Schildhauer et al. 2008).

In plants grown with high nitrogen availability (25 mM), a comparison was made of primary-leaf protein profiles at 16 and 42 d under elevated CO_2 and ambient CO_2 conditions. Analysis of 2-DE gels using PD Quest™ software revealed the presence of a number of spots indicating quantitative differences between elevated CO_2 and ambient CO_2 treatments, and qualitative and quantitative differences as a function of leaf age (16 vs. 42 d) (Table 1). An individual spot was deemed variable if (1) it was present or absent in all three replications; and (2) its density was 1.5 times lower or higher than those of the other gels. A total of 12 differential spots (3, 1003, 3604, 1406, 1505, 5502, 2501, 8501, 1401, 1705, 2101, and 1101) were found to meet these criteria (Table 1). The 12 spots studied were analyzed by MALDI-TOF spectrometry. Proteins were identified using PMF and searching the Uniprot and NCBI databases with the MASCOT algorithm (Matrix Science Ltd., London; http://www.matrixscience.com) (Table 1). Searches revealed that a total of 10 spots (1003, 3604, 1406, 1505, 5502, 2501, 8501, 1401, 1705, and 2101) met the following confidence criteria (Table 1): (1) at least seven peptide matches (7–46); (2) a coverage of at least 15% (24%–72%); and (3) a score of 258 or more (258–1120). The 12 proteins identified coincided with proteins in *Arabidopsis thaliana, Artemisia annua, Ricinus communis, Flaveria bidentis*, *Cucumis sativus*, *Helianthus annuus, Ageratina adenophora*, and *Oryza brachyantha*, *Glycine max*, *Nicotiana tabacum* (Table 1d). The proteins identified by PMF were enzymes belonging to the following functional categories: nucleic acid

binding (At1g76940-spot 3); photosynthesis (Rubisco subunit binding β subunit-spot 3604; Rubisco activase-spots 1406 and 1505; Rubisco large subunit fragment-spot 5502; chloroplasts light harvesting chlorophyll a/b binding protein fragment-spot 1003); energy metabolism (ATP synthase subunit β chloroplastic-spot 2501); photorespiration (serine-hidroxymethyl transferase-spot 8501); foldase protein (peptidyl-prolyl cistrans isomerase chloroplastic-spot 1401); stress response (heat shock protein-spot 1705), and plastid-lipid-associated protein fragment (spot 2101) (Table 1).

As noted earlier, elevated CO_2 concentrations in conjunction with elevated nitrate supply favor sunflower development (Fig. 1), which may account for the increase in photosynthesis-related proteins (spots 3640, 1406, 1505, and 5502) and in energy metabolism proteins (spot 2501); senescence, by contrast, had a negative effect on the latter (Table 1). Elevated CO_2 concentrations and leaf ageing prompted no significant changes in spot intensity for the chloroplast light-harvesting chlorophyll a/b binding protein (spot 1003). Elevated CO_2 concentrations were associated with a drop in serine-hydroxymethyl transferase levels (spot 8501) in both young and senescent sunflower leaves, though levels were higher in senescent leaves, particularly under ambient CO_2 conditions (Table 1). Elevated atmospheric CO_2 concentrations should boost CO_2 photosynthetic fixation to enhance substrate binding of Rubisco (Long et al. 2004; Ainsworth and Rogers 2007), thereby having an adverse impact on the photorespiration process (Bloom 2015). As a result, an increase in atmospheric CO_2 concentrations may alter carbon and nitrogen levels, thus leading to gradual nitrogen decrease; leaves may accumulate carbohydrates faster than the plants are able to acquire nitrogen, prompting a fall in leaf nitrogen content (Reich et al. 2006).

Proteomic analysis revealed that other proteins (Table 1), peptidyl-prolyl cis–trans isomerase (spot: 1401) and plastid-lipid-associated protein (spot: 2101) were unaffected by elevated atmospheric CO_2 concentrations but increased with leaf age. The latter protein (spot 2101) may be synthesized from a SAG, since it is absent from the proteome of young sunflower leaves but present in that of senescent leaves (Table 1). Peptidyl-prolyl cis–trans isomerase (spot: 1401) is a foldase that facilitates protein folding versus stress-induced denaturation; it also regulates the activity of other proteins (Geisler and Bailly 2007). Bissoli et al. (2012) found that peptidyl-prolyl cis–trans isomerases increases tolerance to intracellular acid stress. This protein is designated fibrillin/CDSP34 and the expression of fibrillin/CDtP34 is a response to abiotic stress or developmental stress in various plant organs (Singh and MaNellis 2011).

Conclusions

Elevated CO_2 affects plant growth by modifying the primary metabolism; these changes are closely linked to carbon and nitrogen availability. Under elevated CO_2 (800 $\mu L\ L^{-1}$) and elevated nitrate availability (25 mM) conditions, sunflower primary leaves display an increase in growth, photosynthetic capacity, nitrogen assimilation, and antioxidant defenses compared with plants grown under elevated CO_2 and limited nitrogen availability, thus avoiding senescence progression. Signs of senescence appeared earlier, and were more marked, in plants grown under elevated CO_2 conditions and with limited nitrogen supply (10 mM), suggesting that the induction of senescence process is directly linked to the leaf C/N ratio. These findings add to our understanding of sunflower response to the increasing atmospheric CO_2 levels that contribute to promoting climate change.

Acknowledgements

This work was funded by the Junta de Andalucía (PAI Group BIO-0159). The proteomic analysis was carried out in the UCO-SCAI proteomics facility, a member of Carlos III Networked Proteomics Platform, ProteoRed-ISCI.

References

AbdElgawad, H., Farfan-Vignolo, E.R., de Vos, D., and Asard, H. 2015. Elevated CO_2 mitigates drought and temperature-induced oxidative stress differently in grasses and legumes. Plant Sci. **231**: 1–10. doi:10.1016/j.plantsci.2014.11.001. PMID:25575986.

Aebi, H.E. 1983. Catalase. Pages 273–286 in H.U. Bergmeyer and M. Grassl eds. Methods of enzymatic analysis. Verlag Chemie, Weinheim, Germany.

Agüera, E., Cabello, P., and de la Haba, P. 2010. Induction of leaf senescence by low nitrogen nutrition in sunflower (*Helianthus annuus* L.) plants. Physiol. Plant. **138**: 256–267. doi:10.1111/ppl.2010.138.issue-3. PMID:20051027.

Agüera, E., Ruano, D., Cabello, P., and de la Haba, P. 2006. Impact of atmospheric CO_2 on growth, photosynthesis and nitrogen metabolism in cucumber (*Cucumis sativus* L.) plants. J. Plant Physiol. **163**: 809–817. doi:10.1016/j.jplph.2005.08.010. PMID:16777528.

Ainsworth, E.A., and Rogers, A. 2007. The response of photosynthesis and stomatal conductance to rising [CO_2]: mechanisms and environmental interactions. Plant Cell Environ. **30**: 258–270. doi:10.1111/pce.2007.30.issue-3. PMID:17263773.

Ainsworth, E.A., Rogers, A., Vodkin, L.O., Walter, A., and Schurr, U. 2006. The effects of elevated CO_2 concentration on soybean gene expression. An analysis of growing and mature leaves. Plant Physiol. **142**: 135–147. doi:10.1104/pp.106.086256. PMID:16877698.

Aoyama, S., Reyes, T.H., Guglielminetti, L., Lu, Y., Morita, Y., Sato, T., and Yamaguchi, J. 2014. Ubiquitin ligase ATL31 functions in leaf senescence in response to the balance between atmospheric CO_2 and nitrogen availability in Arabidopsis. Plant Cell Physiol. **55**: 293–305. doi:10.1093/pcp/pcu002. PMID:24399238.

Aranjuelo, I, Cabrerizo, P.M., Arrese-Igor, C., and Aparicio-Tejo, P.M. 2013. Pea plant responsiveness under elevated [CO_2] is conditioned by the N source (N_2 fixation versus NO_3^- fertilization). Environ. Exp. Bot. **95**: 34–40. doi:10.1016/j.envexpbot.2013.06.002.

Bissoli, G., Niñoles, R., Fresquet, S., Palombieri, S., Bueso, E., Rubio, L., Garcia-Sánchez, M.J., Fernandez, J.A., Mulet, J.M., and Serrano, R. 2012. Peptidyl-prolyl cis-trans isomerase

ROF2 modulates intracellular pH homeostasis in Arabidopsis. Plant J. **70**: 704–716. doi:10.1111/tpj.2012.70.issue-4. PMID:22268595.

Bloom, A.J. 2015. Photorespiration and nitrate assimilation: a major intersection between plant carbon and nitrogen. Photosynth. Res. **123**: 117–128. doi:10.1007/s11120-014-0056-y. PMID:25366830.

Bloom, A.J., Burger, M., Rubio Asensio, J.S., and Cousins, A.B. 2010. Carbon dioxide enrichment inhibits nitrate assimilation in wheat and *Arabidopsis*. Science, **328**: 899–903. doi:10.1126/science.1186440. PMID:20466933.

Bloom, A.J., Rubio-Asensio, J.S., Randall, L., Rachmilevitch, S., Cousins, A.B., and Carlisle, E.A. 2012. CO_2 enrichment inhibits shoot nitrate assimilation in C3 but not C4 plants and slows growth under nitrate in C3 plants. Ecology, **93**: 355–367. doi:10.1890/11-0485.1. PMID:22624317.

Bradford, M.M. 1976. A rapid and sensitive method for the quantitation of microgram quantities of protein utilising the principle of protein-dye binding. Anal. Biochem. **72**: 248–254. doi:10.1016/0003-2697(76)90527-3. PMID:942051.

Buchanan-Wollaston, V., Page, T., Harrison, E., Breeze, E., Lim, P.O., Nam, H.G., Lin, J.F., Wu, S.H., Swidzinski, J., Ishizaki, K., and Leaver, C.J. 2005. Comparative transcriptome analysis reveals significant differences in gene expression and signalling pathways between developmental and dark/starvation-induced senescence in Arabidopsis. Plant J. **42**: 567–585. doi:10.1111/tpj.2005.42.issue-4.

Cabello, P., de la Haba, P., González-Fontes, A., and Maldonado, J.M. 1998. Induction of nitrate reductase, nitrite reductase, and glutamine synthetase isoforms in sunflower cotyledons as affected by nitrate, light, and plastid integrity. Protoplasma, **201**: 1–7. doi:10.1007/BF01280705.

Carrion, C.A., Costa, M.L., Martinez, D.E., Mohr, C., Humbeck, K., and Guiamet, J.J. 2013. In vivo inhibition of cysteine proteases provides evidence for the involvement of 'senescence-associated vacuoles' in chloroplast protein degradation during dark-induced senescence of tobacco leaves. J. Exp. Bot. **64**: 4967–4980. doi:10.1093/jxb/ert285. PMID:24106291.

de la Mata, L., Cabello, P., de la Haba, P., and Agüera, E. 2012. Growth under elevated atmospheric CO_2 concentration accelerates leaf senescence in sunflower (*Helianthus annuus* L.) plants. J. Plant Physiol. **169**: 1392–1400. doi:10.1016/j.jplph.2012.05.024. PMID:22818664.

de la Mata, L., de la Haba, P., Alamillo, J.M., Pineda, M., and Agüera, E. 2013. Elevated CO_2 concentrations alter nitrogen metabolism and accelerate senescence in sunflower (*Helianthus annuus* L.) plants. Plant Soil Environ. **7**: 303–308.

de la Haba, P., Cabello, P., and Maldonado, J.M. 1992. Glutamine-synthetase isoforms appearing in sunflower cotyledons during germination. Effects of light and nitrate. Planta, **186**: 577–581. doi:10.1007/BF00198038. PMID:24186788.

Drake, B.G., Gonzalez-Meler, M.A., and Long, S.P. 1997. More efficient plants: a consequence of rising atmospheric CO_2? Ann. Rev. Plant Biol. **48**: 609–639. doi:10.1146/annurev.arplant.48.1.609. PMID:15012276.

Feller, U., Anders, I., and Mae, T. 2008. Rubiscolytics: fate of Rubisco after its enzymatic function in a cell is terminated. J. Exp. Bot. **59**: 1615–1624. doi:10.1093/jxb/erm242. PMID:17975207.

Geisler, M., and Bailly, A. 2007. Tête-à-tête: the function of FKBPs in plant development. Trends Plant Sci. **12**: 465–473. doi:10.1016/j.tplants.2007.08.015. PMID:17826298.

Gorg, A., Postel, W., Domscheit, A., and Gunthe, S. 1988. Two-dimensional electrophoresis with immobilized pH gradients of leaf proteins from barley (*Hordeum-vulgare*): method, reproducibility and genetic-aspects. Electrophoresis, **9**: 681–692. doi:10.1002/(ISSN)1522-2683. PMID:3250872.

Heazlewood, J.L., and Millar, A.H. 2003. Integrated plant proteomics-putting the green genome to work. Funct. Plant Biol. **30**: 471–482. doi:10.1071/FP03036.

Hewitt, E.J. 1966. Sand and water culture methods used in the study of plant nutrition. 2nd ed. Commonwealth Agricultural Bureaux, Farnham Royal, UK.

Intergovernmental Panel on Climate Change (IPCC). 2007. Climate change. *In* S. Solomon, D. Qin, M. Manning, Z. Chen, M. Marquis, K.B. Averyt, M. Tignor, and H.L. Miller, eds. The physical science basis. Contribution of Working Group I to the Fourth Assessment. Report of the Intergovernmental Panel on Climate Change. Cambridge University Press, Cambridge, UK, 996 pp.

Jauregui, I., Aparicio-Tejo, P.M., Avila, C., Cañas, R., Sakalauskiené, S., and Aranjuelo, I. 2016. Root-shoot interactions explain the reduction of leaf mineral content in Arabidopsis plants grown under elevated [CO_2] conditions. Physiol. Plant. doi:10.1111/ppl.12417. PMID:26801348.

Kinsman, E.A., Lewis, C., Davies, M.S., Young, J.E., Francis, D., Vilhar, B., and Ougham, H.J., 1997. Elevated CO_2 stimulates cells to divide in grass meristems: a differential effect in two natural populations of *Dactylis glomerata*. Plant Cell Environ. **20**: 1309–1316. doi:10.1046/j.1365-3040.1997.d01-21.x.

Kontunen-Soppela, S., Parviainen, J., Ruhanen, H., Brosché, M., Keinänen, M., and Thakur, R.C., 2010. Gene expression responses of paper birch (*Betula papyrifera*) to elevated CO_2 and O_3 during leaf maturation and senescence. Environ. Pollut. **158**: 959–968. doi:10.1016/j.envpol.2009.10.008. PMID:19889492.

Lekshmy, S., Jain, V., Khetarpal, S., and Pandey, R. 2013. Inhibition of nitrate uptake and assimilation in wheat seedlings grown under elevated CO_2. Indian J. Plant Physiol. **18**: 23–29. doi:10.1007/s40502-013-0010-6.

Lim, P.O., Kim, H.J., and Nam, H.G. 2007. Leaf senescence. Ann. Rev. Plant Biol. **58**: 115–136. doi:10.1146/annurev.arplant.57.032905.105316. PMID:17177638.

Long, S.P., Ainsworth, E.A., Rogers, A., and Ort, D.R., 2004. Rising atmospheric carbon dioxide: plants FACE the future. Ann. Rev. Plant Biol. **55**: 591–628. doi:10.1146/annurev.arplant.55.031903.141610. PMID:15377233.

Mukherjee, S.P., and Choudhuri, M.A. 1983. Implications of water stress-induced changes in the levels of endogenous ascorbic acid and hydrogen peroxide in *Vigna* seedlings. Physiol. Plant. **58**: 166–170. doi:10.1111/ppl.1983.58.issue-2.

Nakano, Y., and Asada, K. 1981. Hydrogen peroxide is scavenged by ascorbate-specific peroxidase in spinach chloroplast. Plant Cell Physiol. **22**: 860–867.

Nishimura, C., Ohashi, Y., Sato, S., Kato, T., Tabata, S., and Ueguchi, C. 2004. Histidine kinase homologs that act as cytokinin receptors possess overlapping functions in the regulation of shoot and root growth in *Arabidopsis*. Plant Cell, **16**: 1365–1377. doi:10.1105/tpc.021477. PMID:15155880.

Ramagli, L.S., and Rodríguez, L.V. 1985. Quantitation of microgram amounts of protein in two-dimensional polyacrylamide-gel electrophoresis sample buffer electrophoresis. Electroph, **6**: 559–563. doi:10.1002/(ISSN)1522-2683.

Reich, P.B., Hobbie, S.E., Lee, T., Ellsworth, D.S., West, J.B., Tilman, D., Knops, J.M.H., Naeem, S., and Trost, J. 2006. Nitrogen limitation constrains sustainability of ecosystem response to CO_2. Nature, **440**: 922–925. doi:10.1038/nature04486. PMID:16612381.

Riikonen, J., Percy, K.E., Kivimäenpää, M., Kubiske, M.E., Nelson, N.D., Vapaavuori, E., and Karnosky, D.F. 2010. Leaf size and surface characteristics of *Betula papyrifera* exposed to elevated CO_2 and O_3. Environ. Pollut. **158**: 1029–1035. doi:10.1016/j.envpol.2009.07.034. PMID:19674822.

Scheibe, R., and Dietz, K.J. 2012. Reduction-oxidation network for flexible adjustment of cellular metabolism in

photoautotrophic cells. Plant Cell Environ. **35**: 202–216. doi:10.1111/j.1365-3040.2011.02319.x. PMID:21410714.

Schildhauer, J., Wiedemuth, K., and Humbeck, K. 2008. Supply of nitrogen can reverse senescence processes and affect expression of genes coding for plastidic glutamine synthetase and lysine-ketoglutarate reductase/saccharopine dehydrogenase. Plant Biol. **10**: 76–84. doi:10.1111/plb.2008.10.issue-s1. PMID:18721313.

Schippers, J.H.M., Schmidt, R., Wagstaff, C., and Jing, H.C. 2015. Living to die and dying to live: the survival strategy behind leaf senescence. Plant Physiol. **169**: 914–930. doi:10.1104/pp.15.00498. PMID:26276844.

Singh, D.K., and MaNellis, T.W. 2011. Fibrillin protein function: the tip of the iceberg? Trends Plant Sci. **16**: 432–441. doi:10.1016/j.tplants.2011.03.014. PMID:21571574.

Taniguchi, M., and Miyake, H. 2012. Redox-shuttling between chloroplast and cytosol: integration of intra-chloroplast and extra-chloroplast metabolism. Curr. Opin. Plant Biol. **15**: 252–260. doi:10.1016/j.pbi.2012.01.014. PMID:22336038.

Taylor, G., Tricker, P.J., Zhang, F.Z., Alston, V.J., Miglietta, F., and Kuzminsky, E. 2003. Spatial and temporal effects of free-air CO_2 enrichment (POPFACE) on leaf growth, cell expansion, and cell production in a closed canopy of poplar. Plant Physiol. **131**: 177–185. doi:10.1104/pp.011296. PMID:12529526.

Tricker, P.J., Calfapietra, C., Kuzminsky, E., Puleggi, R., Ferris, R., Nathoo, M., Pleasants, L.J., Alston, V., de Angelis, P., and Taylor, G. 2004. Long-term acclimation of leaf production, development, longevity and quality following 3 year exposure to free-air CO_2 enrichment during canopy closure in *Populus*. New Phytol. **162**: 413–426. doi:10.1111/nph.2004.162.issue-2.

Tsukaya, H. 2006. Mechanism of leaf-shape determination. Ann. Rev. Plant Biol. **57**: 477–496. doi:10.1146/annurev.arplant.57.032905.105320. PMID:16669771.

Voss, I., Sunil, B., Scheibe, R., and Raghavendra, A.S. 2013. Emerging concept for the role of photorespiration as an important part of abiotic stress response. Plant Biol. **15**: 713–722. doi:10.1111/plb.2013.15.issue-4. PMID:23452019.

Wang, W., Vignani, R., Scali, M., and Cresti, M. 2006. A universal and rapid protocol for protein extraction from recalcitrant plant tissues for proteomic analysis. Electrophoresis, **27**: 2782–2786. doi:10.1002/(ISSN)1522-2683. PMID:16732618.